Unexpectedly low recombination rates and presence of hotspots in termite genomes

Turid Everitt[1], Tilman Rönneburg[1], Daniel Elsner[2], Anna Olsson[1], Yuanzhen Liu[1], Tuuli Larva[1], Judith Korb[2,3], Matthew T Webster[1,4*]

1) Medical Biochemistry and Microbiology, Uppsala University, Uppsala, Sweden

2) Evolutionary Biology and Ecology, University of Freiburg, Freiburg, Germany

3) Research Institute for the Environment and Livelihoods, Charles Darwin University, Casuarina Campus, Darwin, Australia

4) Science for Life Laboratory, Uppsala University, Uppsala, Sweden

*correspondence to matthew.webster@imbim.uu.se

Abstract

Meiotic recombination is a fundamental evolutionary process that facilitates adaptation and the removal of deleterious genetic variation. Social Hymenoptera exhibit some of the highest recombination rates among metazoans, whereas high recombination rates have not been found among non-social species from this insect order. It is unknown whether elevated recombination rates are a ubiquitous feature of all social insects. In many metazoan taxa, recombination is mainly restricted to hotspots a few kilobases in length. However, little is known about the prevalence of recombination hotspots in insect genomes. Here we infer recombination rate and its fine-scale variation across the genomes of two social species from the insect order Blattodea: the termites *Cryptotermes secundus* and *Macrotermes bellicosus*. We used linkage-disequilibrium-based methods to infer recombination rate. We infer that recombination rates are less than 1 cM/Mb in both species, which is lower than the average metazoan rate. We also observed a highly punctate distribution of recombination in both termite genomes, indicative of the presence of recombination hotspots. We infer the presence of full-length PRDM9 genes in the genomes of both species. We also find that recombination rates in genes are correlated with inferred levels of germline DNA methylation. The finding of low recombination rates in termites indicates that eusociality is not universally connected to elevated recombination rate. We speculate that intense selection among haploid males promotes high recombination rates in social Hymenoptera. This study is one of the first to indicate the presence of PRDM9-based recombination hotspots in an insect genome.

Introduction

Meiotic recombination has two fundamental roles: It is essential for correct disjunction of chromosomes during cell division and it generates new combinations of genetic variants that form the raw material of evolution (Hartfield and Keightley 2012). However, recombination can also be deleterious, as it can generate structural mutations and break up favourable combinations of alleles. Recombination varies among species, with optimal recombination rate in a genome likely determined by the optimal trade-off of its positive and negative evolutionary and mechanistic effects (Stapley et al. 2017).

The highest recombination rates in metazoans observed so far are found in social insects (Wilfert et al. 2007; Stapley et al. 2017). However, until now recombination rate has only been studied in social insects from the order Hymenoptera, to which the majority of social insects belong. Among Hymenoptera, the highest rates are found in the genus *Apis*: the Western honey bee *Apis mellifera* (20.8 cM/Mb) and its relatives *Apis cerana* (17.4 cM/Mb) *Apis florea* (20.8 cM/Mb) and *Apis dorsata* (25.1 cM/Mb) (Beye et al. 2006; Shi et al. 2013; Liu et al. 2015; Wallberg et al. 2015; Rueppell et al. 2016; Kawakami et al. 2019). Other social Hymenoptera also have high rates including the bumblebee *Bombus terrestris* (8.9) (Liu et al. 2017; Kawakami et al. 2019), the stingless bee *Frieseomelitta varia* (9.3 – 12.5 cM/Mb) (Waiker et al. 2021), the wasp *Vespula vulgaris* (9.7 cM/Mb) (Sirviö et al. 2011a) and the ants *Pogonomyrmex rugosus* (11.1 cM/Mb) (Sirviö et al. 2011b) and *Acromymex echinatior* (6.1) (Sirviö et al. 2006). In contrast, the solitary bee *Megachile rotundata* and the solitary wasp *Nasonia* have relatively low rates (1.0 and 1.5 cM/Mb respectively) (Niehuis et al. 2010; Jones et al. 2019). For comparison, the average recombination rate of 15 insect species outside of Hymenoptera is 2.2 cM/Mb (Wilfert et al. 2007).

We can learn about the forces shaping the evolution of recombination rates in general by understanding why high recombination rates have evolved in social Hymenoptera. Several hypotheses have been proposed to explain this observation. One set of explanations focusses on the effects of recombination on intra-colony genetic diversity. For example, increasing the genetic diversity of a colony could promote task specialization among workers (Kent et al. 2012; Kent and Zayed 2013). Similarly, elevated genetic variation in a colony could prevent invasion by pathogens or parasites due to diversification of immune genes (Fischer and Schmid-Hempel 2005). Recombination could also reduce variance in relatedness between nestmates, thereby reducing potential kin conflict within colonies (Sherman 1979; Templeton 1979; Wilfert et al. 2007). Additionally, it has been proposed that high recombination rates could have facilitated the evolution of eusociality over a longer evolutionary timescale, because recombination between genes that take on functions in different castes permits them to evolve more independently (Kent and Zayed 2013). Several studies have addressed these hypotheses (Kent et al. 2012; Liu et al. 2015; Wallberg et al. 2015; Rueppell et al. 2016; Liu et al. 2017; Jones et al. 2019; Waiker et al. 2021; Kawakami et al. 2019) but so far none is strongly supported. It is also not clear whether eusociality *per se* selects for higher recombination rates, or whether high rates are a specific feature of eusocial Hymenoptera.

The main characteristics of eusocial insect species are the presence of a worker caste, which forgo reproduction in order to care for brood of other colony members, and a single (or very few) reproducing individuals (queens, and in termites, also kings). Eusocial insects are found mainly in Hymenoptera, among bees, wasps and ants, and also Blattodea, in which all termites (Infraorder: Isoptera) are eusocial but exhibit varying levels of social complexity. These insect orders likely diverged ~400 million years ago (Misof et al. 2014) and there are substantial differences between social insects from the two orders (Korb 2008; Korb and Thorne 2017). Hymenoptera have haplodiploid sex determination in which males develop from haploid, unfertilized eggs and females derive from diploid, fertilized eggs. In Blattodea, both males and females are diploid. Members of the worker caste in eusocial Hymenoptera are all female, whereas eusocial Blattodea workers are of both sexes. Hymenoptera colonies are headed by one or a small number of queens, whereas Blattodea colonies contain both a king and a queen.

The hypotheses proposed to explain the high recombination rates observed in eusocial Hymenoptera predict that recombination should be elevated in all social insects. However, so far it is unknown whether social insects from other orders also have high rates. As described above, there are fundamental differences in the sex determination system and colony compositions of social insects from Hymenoptera and Blattodea. The robustness of the association between eusociality and high recombination rates can therefore be addressed by assessing mean genomic recombination rates in social Blattodea (termites).

In addition to variation between species, the rate of recombination also varies along chromosomes. In mammals, crossover events are mainly restricted to regions that contain specific motifs that act as binding sites for the PRDM9 (PR/SET domain 9) protein that marks regions for double-stranded breaks, which are repaired by recombination during meiosis (Baudat et al. 2010; Myers et al. 2010; Parvanov et al. 2010). Species with an active PRDM9 include nearly all mammals and many vertebrate taxa (Baker et al. 2017). In species without PRDM9, recombination can be directed to hotspots defined by other features, such as CpG islands and promoters that have open chromatin. Such hotspots have been characterised in

105 the genomes of diverse taxa including yeast, birds, and dogs (Axelsson et al. 2012; Lam and
106 Keeney 2015; Singhal et al. 2015; Berglund et al. 2014). In insects, the prevalence of
107 recombination hotspots is not well studied. Fine-scale recombination maps in the fruit fly
108 *Drosophila melanogaster* and honey bee *A. mellifera* indicate a paucity of recombination
109 hotspots (Chan et al. 2012; Smukowski Heil et al. 2015; Wallberg et al. 2015), whereas
110 hotspots appear to be present in the genome of the butterfly *Leptidea sinapis* (Torres et al.
111 2023).

112 Several other factors may also modulate recombination rate along chromosomes, such as
113 germline DNA methylation. Many species have elevated recombination in CpG islands,
114 which are usually unmethylated in the germline (Axelsson et al. 2012; Lam and Keeney
115 2015; Singhal et al. 2015; Berglund et al. 2014). In insect genomes, methylation is not always
116 present, but commonly restricted to gene bodies (Arsala et al. 2022; Wang et al. 2013; Lyko
117 et al. 2010; Ventós-Alfonso et al. 2020; Bewick et al. 2019; Harrison et al. 2018). In the
118 honey bee *A. mellifera* and solitary bee *M. rotundata* recombination is reduced in genes,
119 and particularly in those inferred to have the highest levels of germline methylation
120 (Wallberg et al. 2015; Jones et al. 2019). In addition, some studies have identified
121 correlations between caste-biases in gene expression and recombination. In honey bees,
122 genes with worker-biased gene expression have been found to have elevated recombination
123 rates (Kent et al. 2012) but this is likely an indirect result of differences in germline
124 methylation between sets of genes (Wallberg et al. 2015).

125 Here we estimate recombination rate and its fine-scale variation across the genomes of two
126 distantly related termite species with contrasting social complexities (Korb and Hartfelder
127 2008; Korb and Thorne 2017). The drywood termite *Cryptotermes secundus* (Kalotermitidae)
128 has a low level of social complexity. Its colonies consist of a few hundred individuals and
129 totipotent workers from which queens and kings develop (Hoffmann et al. 2012). It belongs
130 to the wood-dwelling (one-piece nesting) termites that nest in a single piece of wood that
131 also serves as their food source. *Macrotermes bellicosus* (Termitidae: Macrotermitinae) is a
132 fungus-growing termite with a high level of social complexity, with colonies of several
133 millions of individuals and sterile workers. It belongs to the foraging (multiple-pieces
134 nesting) termites, where workers leave the nest to forage for food.

135 The study has three main aims. Firstly, we aim to test the robustness of the association
136 between sociality and high recombination rate. If sociality is a universal driver of high
137 recombination rates, we would expect both termite species to have elevated recombination
138 rates, and that it is particularly elevated in *M. bellicosus*, which has a higher level of social
139 complexity. Secondly, we aim to determine whether recombination hotspots exist in the
140 two termite genomes, and infer whether active full-length PRDM9 genes are present in their
141 genomes. Thirdly, we aim to analyse the factors that govern variation in recombination
142 across the genome. In particular, whether genomic variation in recombination rates is
143 associated with patterns of methylation and gene expression as has been reported in other
144 studies.

145 To perform the analysis, we conducted whole-genome sequencing of 10 samples each of *C.*
146 *secundus* and *M. bellicosus*, randomly sampled from different colonies. We then used
147 patterns of SNP variation to infer fine-scale variation in recombination rate across the
148 genomes using coalescent-based analysis of patterns of linkage disequilibrium. Our results
149 indicate unexpectedly low rates of recombination in both termite genomes, demonstrating
150 that sociality is not universally associated with high recombination rates as proposed from

151 analysis of social Hymenoptera. They also suggest the presence of recombination hotspots,
152 which may be controlled by the PRDM9 protein.

153

154 **Results**

155 *Genetic variation in two termite species is typical for social insects*

156 We utilized genome assemblies of two termite species: *C. secundus* and *M. bellicosus*. The
157 genome assembly of *C. secundus* (Csec_1.0) (Harrison et al. 2018) is divided into 55,483
158 scaffolds with a scaffold N50 of 1.2 Mbp and a total length of 1.0 Gbp. The genome
159 assembly of *M. bellicosus* (Qiu et al. 2023) is 1.3 Gbp in total length across 275 scaffolds with
160 scaffold N50 of 22.4 Mbp.

161 We sequenced 10 unrelated individuals each of *C. secundus* and *M. bellicosus* to a mean
162 depth of 34x and 31x per sample, respectively (Supplementary Table S1). We mapped reads
163 to the appropriate genome assemblies and called variants in each species. In *C. secundus* we
164 called 15.1 million SNPs and in *M. bellicosus* 5.6 million SNPs (Table 1). One individual of *C.*
165 *secundus* (CS_8) was excluded due to a low proportion of mapped reads, poor mapping
166 quality and strand bias in mapping. Estimates of variation based on θ_W (Watterson 1975) are
167 0.14% and 0.44% in *M. bellicosus* and *C. secundus* respectively, which are broadly
168 comparable to levels of variation in the honey bee *A. mellifera* (0.3 - 0.8%) (Wallberg et al.
169 2014).

170 We used these estimates of genetic variation to estimate effective population size (N_E) for
171 each of the sampled populations. These rely on an estimate of mutation rate, μ, in each
172 species. As there is no estimate of μ for Blattodea, we considered a range of estimates from
173 Diptera (*Drosophila*) (Keightley et al. 2009, 2014), Hymenoptera (bumblebee (Liu et al. 2017)
174 and honey bee (Yang et al. 2015)) and Lepidoptera (Keightley et al. 2015) that range
175 between 2.8 - 3.5 x 10^{-9} $bp^{-1}gen^{-1}$(Table 1).

176 Our estimates of N_E based on θ_W are 98,600 – 123,300 in *M. bellicosus*, which has high social
177 complexity, and 314,900 – 393,700 in *C. secundus*, with lower level of social complexity. This
178 is consistent with previous evidence that eusocial species with large colonies and high social
179 complexity tend to have lower effective population sizes and the values are broadly
180 comparable to levels of N_E found in social and solitary Hymenoptera (Leffler et al. 2012;
181 Romiguier et al. 2014).

182 *Low average recombination rate in termite genomes*

183 We next examined the decay of linkage disequilibrium (LD) based on the statistic r^2. Both
184 termite species show more extensive LD compared to *A. mellifera*, which has an extremely
185 high recombination rate (Wallberg et al. 2015) (Figure 1). As N_E is broadly similar in all these
186 species, these differences are expected to largely represent differences in recombination
187 rates, and indicate that the two termite species do not exhibit the elevated genome average
188 recombination rate that is observed in honey bees.

189 We estimated variation in the population recombination rate, ρ, in both datasets using
190 LDhat (Auton and McVean 2007) (Table 1). Average rates of ρ/kb are 1.7 and 4.8 in *M.*
191 *bellicosus* and *C. secundus* respectively. These estimates can be converted to cM/Mb using
192 estimates of N_E, which gives estimates of average recombination rate of 0.34 - 0.43 cM/Mb
193 in *M. bellicosus* and 0.31 - 0.38 cM/Mb in *C. secundus*, which is much lower than the

194 average among insects (Stapley et al. 2017), and particularly lower than the elevated
195 recombination rates inferred in eusocial Hymenoptera. This represents the first estimation
196 of recombination rate in social insects outside of Hymenoptera and demonstrates that
197 eusociality is not a universal driver of high recombination rates.

198 *Evidence for active recombination hotspots in termite genomes*

199 Variation in recombination rate across the genome in *C. secundus* and *M. bellicosus* appears
200 highly variable (Figure 2). We characterised the distribution of recombination events across
201 the two termite genomes using cumulative distribution plots (Figure 3). We found that 50%
202 of the recombination occurs in 4.8% of the genome in *C. secundus* and 3.5% of the genome
203 in *M. bellicosus*. This indicates that the majority of recombination events are restricted to a
204 much smaller portion of the genome than observed in *A. mellifera*, where 50% of
205 recombination events occur in >30% of the genome (Wallberg et al. 2015).

206 We further investigated whether recombination hotspots are present in the two termite
207 genomes by looking at the distribution of ρ in windows of 1 kbp, 10 kbp and 100 kbp across
208 the genome (Figure S1). For all window sizes, a small subset of windows was observed with
209 ρ greatly exceeding the mean in both termite species. For example, the percentage of 1 kbp
210 windows with recombination rate at least four standard deviations above the genome wide
211 mean value is 1.20% for *C. secundus* and 0.88% for *M. bellicosus*. By contrast, *A. mellifera*
212 has no windows above this limit for any window size, consistent with a lack of
213 recombination hotspots.

214 We next defined hotspots as 2 kbp regions with more than 5-fold higher recombination rate
215 than the local background as defined as the surrounding 100 kbp and used STREME (Bailey
216 2021) to identify 8 to 20-mers that were enriched in hotspots compared to the rest of the
217 genome. This yielded significantly enriched motifs in both species (12 motifs for *C. secundus*
218 and 8 motifs for *M. bellicosus*, after multiple testing; Table S2 and S3). However, none the
219 motifs we identified are present in more than 5% of hotspots and exhibit more than 2-fold
220 difference relative to the background, suggesting they are not viable candidate motifs for
221 promoting recombination in hotspots.

222 *Identification and characterization of the PRDM9 gene in termites*

223 We searched the *C. secundus* and *M. bellicosus* genomes for evidence of complete PRDM9
224 genes, which could potentially govern the presence of recombination hotspots in these
225 genomes. The *C. secundus* genome contains a PRDM9 homolog (XP_023708049.2) with
226 annotated KRAB, SSXRD, SET and zinc finger domains (Figure 4). It is plausible that this gene
227 is responsible for initiation of recombination in hotspots as it does in many other taxa. There
228 is no complete homolog of PRDM9 in the *M. bellicosus* annotation. We therefore used
229 BLAST to search for sequences homologous to the conserved functional domains from *C.*
230 *secundus*. We identified a putative PRDM9 orthologue on Scaffold 42, containing all
231 domains in the correct order. However, we also identified retroviral conserved domains 5' of
232 the zinc-finger domains in this gene in the *M. bellicosus* genome assembly.

233 We used a zinc-finger prediction algorithm (Persikov and Singh 2014) to predict DNA binding
234 motifs from the zinc-finger domain present in PRDM9 in the *C. secundus* and *M. bellicosus*
235 genome assemblies, for which an accurate annotation was available. The most probable
236 consensus motifs were TAATAAGTAGAATCGTTTAG and
237 TATGGAACGACAGGAACAACGACATCATCAGCCGCCTAAT for *C. secundus* and *M. bellicosus*

238 respectively. Base probability matrices for these motifs are shown in Table S4. We tested
239 whether the presence of these motifs corresponded to elevated recombination considering
240 1 kbp around the motif. However, recombination rate was not significantly elevated around
241 these predicted motifs for either species, either when searching based on the most likely
242 motif, or by searching based on the probability matrices.

243 *Genomic correlates of recombination rate*

244 We analysed genomic correlates of recombination rate in 10 kbp windows. There is a
245 significant correlation between recombination and $CpG_{O/E}$ in both species with Spearman's
246 $\rho = 0.10$, $p < 1 \times 10^{-4}$ for *C. secundus* and Spearman's $\rho = 0.24$, $p < 1 \times 10^{-4}$ for *M. bellicosus*
247 (Figure S2). A reduction of recombination rates in regions of low CpG content is consistent
248 with interference of germline methylation with recombination. However, as the correlation
249 coefficients are low, the explanatory power is weak. Correlations of similar magnitudes were
250 observed between recombination and GC content (Spearman's ρ =0.23 for *C. secundus*, p <
251 1×10^{-4}, and Spearman's ρ =0.017 for *M. bellicosus*, $p < 1 \times 10^{-4}$). This correlation has been
252 associated with an effect of recombination in driving GC through GC biased gene conversion
253 but the relatively low correlation coefficients indicate that this force is not strong in
254 termites. By contrast, the correlation between GC content and recombination rate is much
255 stronger in honey bee ($R^2 = 0.506$), which is likely caused by high recombination rates and
256 intense GC-biased gene conversion (Wallberg et al. 2015).

257 There is no significant correlation between overall repeat element density and
258 recombination rate in either of the two genomes. There is a weak positive but highly
259 significant correlation between simple repeats and recombination in both genomes
260 (Spearman's $\rho = 0.07$, $p < 1 \times 10^{-4}$ for *C. secundus* and Spearman's $\rho = 0.06$, $p < 1 \times 10^{-4}$ for
261 *M. bellicosus*). SINE and LINE elements are also only weakly associated with recombination
262 rate in both genomes (SINEs: Spearman's $\rho = 0.02$, $p < 1 \times 10^{-4}$ for *C. secundus* and
263 Spearman's $\rho = -0.01$, $p > 0.05$ for *M. bellicosus*; LINEs: Spearman's $\rho = 0.001$, $p > 0.05$ for *C.*
264 *secundus* and Spearman's $\rho = -0.01$, $p < 1 \times 10^{-4}$ for *M. bellicosus*). There is a significant
265 negative correlation between gene density and recombination for the *M. bellicosus* genome
266 (Spearman's $\rho = -0.20$, $p < 1 \times 10^{-4}$), but no significant correlation for *C. secundus*. We also
267 tested whether hotspots differ from the background with respect to GC content. The GC
268 content does not differ substantially between hotspots and the rest of the genome in either
269 species (means of 40.1% and 40.4% for *M. bellicosus* and 40.5% in both categories for *C.*
270 *secundus*).

271 We found a highly significant correlation between nucleotide diversity (π) and
272 recombination in both species (Figure S2), with Spearman's $\rho = 0.32$, $p < 1 \times 10^{-4}$ for *C.*
273 *secundus* and Spearman's $\rho = 0.52$, $p < 1 \times 10^{-4}$ for *M. bellicosus*. This correlation is found
274 across a wide range of eukaryotic taxa and is generally accepted to be caused by the
275 interaction between recombination and linked selection (Nachman 2001; Begun and
276 Aquadro 1992).

277 *Recombination and gene expression patterns correlate with $CpG_{O/E}$*

278 Analysis of the distribution of $CpG_{O/E}$ in both termite species showed that it is bimodally
279 distributed, with substantially lower values in introns and exons compared to flanking
280 noncoding regions (Figure S3). This indicates that germline DNA methylation is biased
281 towards gene bodies in the two termite genomes, a pattern that is also found in honey bees

282 and other insect genomes with functional DNA methylation (Harrison et al. 2018; Elango et
283 al. 2009; Sarda et al. 2012). We found that exons have lower $CpG_{O/E}$ compared to introns,
284 which are both lower than flanking regions (Figure 5, top row; all comparisons $p < 0.001$
285 after Bonferroni correction) consistent with higher levels of germline methylation in exons
286 (Table S5). We next analysed how recombination rate varies among genomic features. We
287 found that ρ/kbp is also significantly reduced in genes compared to flanking regions, with
288 exons showing reduced ρ/kbp compared to introns (Figure 5, bottom row, all p-values
289 <0.005 after Bonferroni correction). This effect was seen in both species and is more
290 pronounced for *C. secundus* than for *M. bellicosus.* There was a significant correlation
291 between $CpG_{O/E}$ and recombination rate among genes (Spearman's $\rho = 0.166$, $p < 1 \times 10^{-4}$ for
292 *C. secundus* and $\rho = 0.369$, $p < 1 \times 10^{-4}$ for *M. bellicosus*).

293 We next investigated whether patterns of gene expression between castes and sexes
294 (hereafter, for short 'caste-biased gene expression') were correlated with $CpG_{O/E}$ and
295 recombination rate using gene expression data from two studies (Lin et al. 2021; Elsner et
296 al. 2018). It has been proposed that it is evolutionarily advantageous for genes with worker-
297 biased expression to be located in regions with elevated recombination (Kent et al. 2012).
298 For *C. secundus*, worker-biased and queen-biased genes were identified (Lin et al. 2021). For
299 *M. bellicosus*, we defined several categories based on gene expression difference among
300 castes (Elsner et al. 2018). The categories we used were queen-biased, king-biased, worked-
301 biased, male-biased, female-biased, reproduction-biased, and differentially expressed (see
302 methods for details). Comparisons of $CpG_{O/E}$ and recombination rate for the original gene
303 expression categories reported for *M. bellicosus* are shown in Figure S4. We find that mean
304 $CpG_{O/E}$ in gene bodies shows significant variation between gene expression categories in
305 both *M. bellicosus* and *C. secundus* (Figure 6). However, this variation is not consistent
306 between species. In *M. bellicosus*, queen-biased and female-biased genes have low $CpG_{O/E}$
307 and king-biased and male-biased genes have high $CpG_{O/E}$. In *C. secundus*, queen-biased
308 genes have higher than average $CpG_{O/E}$.

309 The differences in $CpG_{O/E}$ between caste-biased gene expression categories are mirrored by
310 differences in ρ/kbp (Figure 6). Gene expression categories with elevated $CpG_{O/E}$
311 consistently show elevated ρ/kbp, and this pattern is found in both species. Studies in the
312 honey bee have found that worker-biased genes have lower CpG and higher recombination
313 rates (Kent et al. 2012; Wallberg et al. 2015). In *M. bellicosus,* we find that worker-biased
314 genes have slightly elevated $CpG_{O/E}$ and ρ/kbp. However, in *C. secundus*, these values are
315 reduced in worker-biased genes, whereas queen-biased genes have a slightly elevated
316 $CpG_{O/E}$ and ρ/kbp in this species.

317 We investigated the relative roles of $CpG_{O/E}$ and gene expression in determining ρ in genes
318 using a linear model, with $CpG_{O/E}$, ρ in flanking region and expression categories as
319 explanatory variables. In both *C. secundus* and *M. bellicosus*, we found that $CpG_{O/E}$ was the
320 strongest predictor of recombination rate variation among genes (Tables S6 and S7) in line
321 with the analyses above. We found that caste-biased expression had no significant impact
322 on the recombination rate, with the exception of king-biased genes in *M. bellicosus*. These
323 have higher ρ/kbp than expected based on $CpG_{O/E}$ alone. Generally, $CpG_{O/E}$ is a good
324 predictor of ρ/kbp, and the variation in ρ/kbp among expression categories likely mainly
325 reflects differences in $CpG_{O/E}$, as accounting for it removes most significant interactions.

326

Discussion

The main findings we present here are 1) that two distantly related termite species with varying social complexity both have relatively low genomic average rates of meiotic recombination, 2) both genomes possess recombination hotspots and likely contain full-length copies of PRDM9 and, 3) there are reduced levels of recombination in genes and genome regions depleted in CpG sites. Our findings contrast with the extremely elevated recombination rates observed in eusocial Hymenoptera, which are likely to be generated by a feature that is specific to these taxa. The finding of recombination hotspots is one of the first in insects. This could reflect a conserved function of PRDM9 in recombination in vertebrates and invertebrates. Our results also support a role for germline methylation in suppressing recombination.

Eusociality is not a universal driver of high rates of meiotic recombination

Elevated genomic rates of recombination are characteristic of all eusocial Hymenoptera so far investigated. Several hypotheses have been advanced to explain this phenomenon, which are all based on an evolutionary advantage of recombination in eusocial species (Wilfert et al. 2007). For instance, it has been suggested that elevated recombination could increase genetic diversity in a colony. This could promote diversity in the workforce, enabling more efficient task specialisation among workers (Kent et al. 2012). Alternatively, it could render the colony less susceptible to invasion by parasites and pathogens (Fischer and Schmid-Hempel 2005). Elevated recombination might also favour rapid evolution of caste-specifically expressed genes (Kent and Zayed 2013). In addition, increased recombination could lead to reduced variance in relatedness, which could prevent kin conflict in colonies (Sherman 1979; Templeton 1979).

All these hypotheses predict that recombination rate should be elevated in all eusocial insects. Here, however, in the first report of recombination rate in social insects outside of Hymenoptera, we find overall low levels of recombination. Both termite species studied here are eusocial, and in particular *M. bellicosus* has extremely large and complex colonies characteristic of eusociality (Korb and Thorne 2017). The low recombination rate inferred in the two termite genomes prompts re-evaluation of hypotheses connecting eusociality with high recombination rates. Although both termites and social Hymenoptera share many traits, they differ in others that reflect their different ancestries.

The chromosome numbers of both termite species (*M. bellicosus*, 2n = 42 and for *C. secundus*, 2n = 40) are typical for termites, although variation exists between taxa (Jankásek et al. 2021). These values do not differ from those observed in Hymenoptera, which have a similar range (e.g. *A. mellifera*, 2n = 32) and do not vary between solitary and eusocial taxa (Cardoso et al. 2018; Cunha et al. 2021; Ross et al. 2015). This suggests that differences in chromosome number are unlikely to be relevant in explaining the differences in recombination rates among these taxa.

One proposed advantage of sex and recombination is that it is associated with sexual selection and a higher intensity of selection on males. This could be advantageous because differential male mating success can reduce mutational load in sexual populations by causing deleterious mutations to segregate at a lower equilibrium frequency on average (Siller 2001; Agrawal 2001). Recombination is essential for effective purging of deleterious alleles as it unlinks deleterious variants from nearby beneficial ones thus preventing selection interference (Hartfield and Keightley 2012). Selection has been found to be

stronger in males than females across animal species (Janicke et al. 2016; Winkler et al. 2021). Species with a male-biased sex ratio are expected to experience particularly intense selection on males. It is therefore possible that recombination rate could be particularly elevated in species in which males face intense competition as this increases the evolutionary advantage of recombination.

The genus *Apis* produces highly male-biased reproductive offspring and thousands of male drones compete to fertilise a small number of female queens (Winston 1991; Koeniger et al. 2011; Baer 2005). It is also in this genus that the most extreme recombination rates have been inferred (Beye et al. 2006; Shi et al. 2013; Liu et al. 2015; Wallberg et al. 2015; Rueppell et al. 2016; Kawakami et al. 2019). Male-biased sex ratios are also observed in other social bees and wasps. Both male and female biased operational sex ratios have been observed in ants, but are difficult to measure because workers invest more resources in female offspring and may manipulate sex ratios. In non-social Hymenoptera, females lay roughly equal numbers of haploid and diploid eggs (Trivers and Hare 1976). The sex ratio of reproductive males and females is also relatively even in most termite species (Roisin 2001). It is possible that the male-biased sex ratio observed in many eusocial Hymenoptera could favour elevated recombination rates in the species so far studied.

The effects of higher intensity of selection on males on recombination rate could be even more pronounced when males are haploid as in Hymentoptera. Haploid males can be considered analogous to the gametes of females. However, as many more genes are expressed in adult haploid males compared to gametes there are more targets of selection. Selection against deleterious alleles is particularly effective in haploid males because recessive deleterious alleles are exposed (Hedrick and Parker 1997).

Although its effects on overall recombination rates are unclear, haploid selection is believed be key to driving sex-specific differences in recombination rate (Immler 2019). It has been argued that differences in the intensity of selection between sexes in the haploid phase can drive differences in recombination rates between sexes among animal and plant species (heterochiasmy) (Burt et al. 1991; Trivers 1988; Lenormand 2003; Lenormand and Dutheil 2005). It is unclear how theory and observations regarding the prevalence and nature of heterochiasmy applies to haplodiploids, in which only females recombine. However, it appears that the intensity of selection on the haploid phase likely has the potential to drive selective pressure on recombination rates.

Further research is needed to determine the cause of variation in recombination rates among social and non-social insects. For example, simulations could be used to determine the effect of selection on haploid males on recombination rates, considering different sex ratios. In addition, it is necessary to estimate recombination rate in a wider range of social and non-social species to determine whether the strength of selection on males is a key factor in determining these rates.

Full length PRDM9 gene and recombination hotspots in termite genomes

Our results are also indicative of the presence of recombination hotspots in the two termite genomes. The fine-scale distribution of recombination rate in both termite genomes is similar to that in humans where 50% of recombination events occur in ~6% of the genome (Myers et al. 2005). This contrasts to the honey bee and solitary bees where fine-scale maps are available and recombination is relatively uniformly distributed in the genome (Wallberg et al. 2015; Jones et al. 2019).

417 Two main mechanisms have been shown to lead to recombination hotspots. The first, which
418 is best understood in human and mouse, is governed by the PRDM9 protein. A zinc-finger
419 domain recognises a specific DNA sequence motif and then performs a histone modification
420 in the vicinity, which marks the sequence for a DNA double-stranded break that is repaired
421 by recombination during meiosis (Baudat et al. 2010; Myers et al. 2010; Parvanov et al.
422 2010). In species with this mechanism, the zinc finger domain is fast evolving, which results
423 in a rapid turnover of hotspot locations (Myers et al. 2010). Full-length PRDM9 orthologues
424 are present among a range of highly-diverged vertebrates including many fish, reptiles and
425 mammals, but many full or partial losses of the gene have also been inferred. In a study of
426 225 vertebrate genomes, a minimum of six partial and three complete losses were inferred
427 (Baker et al. 2017). However, it is unclear whether PRMD9-hotspots are common in
428 invertebrates.

429 A second mechanism is found in vertebrates that lack PRDM9, in which recombination
430 hotspots are localised to regions of open chromatin such as CpG islands and promoters. This
431 is found in dogs and in most or all birds, in which PRDM9 has been lost, and results in
432 hotspots with stable rather than rapidly evolving locations (Axelsson et al. 2012; Singhal et
433 al. 2015). A similar pattern is also observed in the yeast *Saccharomyces cerevisiae* in which
434 recombination preferentially occurs in promoter regions (Wu and Lichten 1994). In
435 invertebrates such as *Drosophila* and *Caenorhabditis elegans*, recombination hotspots
436 appear to be absent (Coop and Przeworski 2007; Chan et al. 2012; Smukowski Heil et al.
437 2015). Fine-scale maps of bees have also not revealed recombination hotspots (Wallberg et
438 al. 2015; Jones et al. 2019).

439 We find evidence that recombination is directed towards hotspots in both termite species.
440 We also identify a full-length PRDM9 gene in both species, containing all of the domains
441 needed to initiate recombination. However, we are unable to demonstrate that PRMD9 is
442 responsible for the presence of recombination hotspots in the two genomes. We used a
443 motif prediction algorithm to predict the zinc-finger binding motif in the *C. secundus*
444 genome, but we did not observe elevated recombination rate around instances of the motif
445 in the genome. Furthermore, we did not identify any common sequence motifs that were
446 enriched in recombination hotspots in either of the termite genomes. A plausible
447 interpretation of these observations is that the PRDM9 protein indeed initiates
448 recombination in hotspots in both species, but that positive selection leads to frequent
449 shifts in the target motifs, which results in a lack of a strong association between a specific
450 motif and LD-based hotspots (Myers et al. 2010). It is also possible that the sequences of the
451 zinc-finger motifs are not correctly represented in the genome assemblies, which could
452 result from problems with assembly around minisatellites. However, an unknown
453 mechanism could also be responsible for hotspots in termites.

454 *Evidence that germline DNA methylation suppresses recombination*

455 In insects with a functioning DNA methyltransferase machinery, the $CpG_{O/E}$ statistic shows
456 substantial variation along the genome, which mainly reflects variation in levels of germline
457 DNA methylation (Elango et al. 2009). In contrast to vertebrate genomes, methylation is
458 strongly skewed towards gene bodies in the genomes of insects (Glastad et al. 2011). The
459 overall genomic correlation between $CpG_{O/E}$ and recombination rate is significant but weak
460 in the two termite genomes. This could reflect that the majority of the genomes are not
461 methylated, so that much of the variation in $CpG_{O/E}$ on the genome scale is not strongly
462 influenced by methylation. In the two termite genomes studied here, we find lowest values

463 of $CpG_{O/E}$ in exons, whereas noncoding flanking regions are biased towards higher values,
464 indicative of lower levels of DNA methylation (Figure 5, Figure S3). All categories display a
465 predominantly bimodal distribution of $CpG_{O/E}$, likely reflective of the presence of
466 methylated and unmethylated regions. The differences in $CpG_{O/E}$ are also reflected by
467 differences in recombination rate (ρ/kb), which are reduced in regions inferred to be more
468 highly methylated.

469 Using linear models, we identified $CpG_{O/E}$ as the factor with the strongest influence on
470 recombination rate variation among genes, consistent with an effect of DNA methylation on
471 recombination rate. This factor had a stronger effect than differences in gene expression
472 patterns across castes, a result that was also observed in the honey bee genome (Wallberg
473 et al. 2015). This indicates that recombination rate variation is not modulated by differences
474 in gene expression in these genomes, which might be expected if natural selection favours
475 increased recombination rates in certain genes. For example, it has been proposed that
476 natural selection could favour elevated recombination rates in genes with roles in worker
477 behaviour or in immune function due to their important roles in colony function (Wilfert et
478 al. 2007; Kent et al. 2012). However, the results presented here suggest that differences in
479 recombination rate between genes with caste-biased patterns of gene expression are mainly
480 due to underlying differences in methylation levels among genes.

481 A direct effect of germline DNA methylation in suppressing recombination could explain
482 variation in recombination landscapes among vertebrates and invertebrates. Vertebrate
483 genomes are usually highly methylated with the exception of CpG islands. In the absence of
484 a functional PRDM9 gene, recombination events tend to localise to CpG islands in vertebrate
485 genomes (for example in dogs and birds)(Singhal et al. 2015; Axelsson et al. 2012). However,
486 in insect genomes without PRDM9, which are typically not as highly methylated,
487 recombination events do not cluster in hotspots (for example in fruit flies and honey bees)
488 (Chan et al. 2012; Wallberg et al. 2015). However, in the presence of a functional PRDM9 in
489 both vertebrate or invertebrate genomes, recombination tends to cluster in hotspots
490 determined by sequence motifs.

491 *Conclusion*

492 We find low rates of meiotic recombination in the genomes of two termite species from
493 disparate parts of the phylogeny and with contrasting social complexity. This demonstrates
494 that eusociality is not a universal driver of high recombination rates. We propose a haploid
495 selection hypothesis that could potentially explain why recombination might be elevated in
496 eusocial Hymenopterans, but not other social insects. This hypothesis predicts that
497 recombination rates should depend on the intensity of selection in the haploid stage of the
498 life cycle, but requires theoretical and empirical testing. We also provide evidence that
499 recombination is biased towards hotspots in both genomes, and that they both contain full-
500 length PRDM9 genes. The results are consistent with the involvement of PRDM9 in initiating
501 recombination in hotspots in termites, and they are one of the first indications of the
502 existence of this mechanism in invertebrates. Additional studies are required to
503 demonstrate a role of PRDM9 in initiating recombination in hotspots in termites.

504

505 **Materials and Methods**

506 *Sample collection*

507 *Cryptotermes secundus* colonies were collected from dead *Ceriops tagal* mangrove trees
508 near Palmerston-Channel Island (Darwin Harbor, Northern Territory, Australia; 12°30'S
509 131°00'E). Colonies were then kept in *Pinus radiata* wood blocks in climate rooms in
510 Germany, providing 28 °C, 70% relative humidity, and a 12-h day/night cycle (Lin et al.
511 2021). *Macrotermes bellicosus* samples were collected from colonies in Kakpin, next to the
512 Comoé National Park in Côte d'Ivoire (coordinates 8°39'N 3°46'W) (Elsner et al. 2018). For
513 both species, each of the sequenced samples came from a different colony.

514 *Population sequencing*

515 The termites were cut in two, approximately between head and thorax. DNA was extracted
516 from both parts using the QIAGEN Blood and Tissue Kit following the standard protocol,
517 including treating with 4 µL RNase and 25 µL Proteinase K. The DNA extraction product was
518 cleaned and concentrated with ZymoResearch Genomic DNA Clean & Concentrator kit. For
519 most samples, the RNase treatment was repeated prior to cleaning and concentrating. One
520 DNA sample from each individual was chosen, based on the DNA amount and quality, to be
521 sequenced. We performed Illumina short-read sequencing using NovaSeq 6000 with 2 x 150
522 bp paired end reads.

523 *Read mapping and variant calling*

524 The sequence data from the two termite species were mapped to the reference genomes
525 for *C. secundus* (Csec_1.0) (Harrison et al. 2018) and *M. bellicosus* (Qiu et al. 2023),
526 respectively, using Burrows-Wheeler alignment tool BWA version 0.7.17 (Li & Durbin 2009)
527 with the BWA-MEM algorithm. Sorting and indexing of the BAM-files was done with the
528 Samtools package version 1.17 (Li et al. 2009), followed by adding read groups and marking
529 duplicate reads with Picard toolkit version 1.118 (http://broadinstitute.github.io/picard/).
530 After mapping, we excluded all scaffolds < 1kb from the *C. secundus* genome, which in total
531 correspond to 2% of the genome size, as they are potentially of lower quality and not
532 informative for analysis of linkage disequilibrium or recombination. For *M. bellicosus* there
533 are no scaffolds shorter than 1 kbp, but we excluded the following five scaffolds, which
534 together correspond to 3.78% of the genome length, due to unexpectedly high
535 heterozygosity: 93, 62, 41, 35 and 32.

536 One of the *C. secundus* individuals did not map well to the reference genome (71% mapped
537 reads, unequal distribution between forward and reverse strand and an average mapping
538 quality of 35 while all the other samples had an average mapping quality >45). This
539 individual was excluded from all further analyses and hence the total number of termite
540 individuals analysed in this study is 19, out of which 9 were *C. secundus*.

541 Variant calling was done using the tools HaplotypeCaller, GenomicsDBImport and
542 GenotypeGVCFs from GATK version 4.3.0.0 as described in their best practices workflow
543 (https://gatk.broadinstitute.org/hc/en-us/articles/360035535932-Germline-short-variant-
544 discovery-SNPs-Indels-, last accessed 2023-07-11). The variants were filtered in multiple
545 steps, first removing extended regions of low mapping quality or deviating read depth as
546 those regions are likely to be unreliable. This was done based on statistics from the
547 Samtools mpileup and depth tools, respectively, removing 100 kb windows with mean
548 mapping quality below 70 or mean read depth more than two standard deviations from the
549 genome-wide mean. In the later recombination rate and LD decay calculations, values in
550 intervals spanning those regions were also removed. Indels were removed using VCFtools
551 version 0.1.16 (Danecek et al. 2011) before GATK VariantFiltration was run with the

552 following limits, which are all equal to or stricter than the ones recommended
553 (https://gatk.broadinstitute.org/hc/en-us/articles/360035890471-Hard-filtering-germline-
554 short-variants, last accessed 2023-07-11) and adapted to the observed distributions of the
555 corresponding statistics: QD<2; FS>50; MQ<40; ReadPosRankSum< -4; ReadPosRankSum>4;
556 SOR>3; ExcessHet>5 for both species as well as MQRankSum with limits -5 and 5 for *C.*
557 *secundus* and limits -6 and 4 for *M. bellicosus*. This was followed by additional filtering with
558 VCFtools to select only bi-allelic sites with a minimum quality score of 30 and maximum of
559 40% missing genotypes. The SNPs with mean read depth in the lowest or highest 2.5% of the
560 depth distribution were also filtered out, which translates to a depth below 10 or above 34
561 for *C. secundus* and below 5 or above 40 for *M. bellicosus.* For the recombination rate
562 calculations, the SNPs were also filtered for a minor allele count >= 2, as rare variants
563 appearing on only one chromosome are difficult to distinguish from errors and are not
564 informative regarding LD. The data was also phased and imputed using Beagle version 5.1
565 (Browning and Browning 2007; Browning et al. 2018).

566 *Estimation of LD decay*

567 The decay of linkage disequilibrium, r2, with increasing physical distance was estimated with
568 the software PopLDDecay version 3.42 (Zhang et al. 2019) over a maximum distance of 10
569 kbp. For this analysis, sequence data from *A. mellifera scutellata* was included for
570 comparison ((Wallberg et al. 2017); BioProject PRJNA357367). The *A. m. scutellata*
571 sequences were mapped to the Amel_HAv3.1 reference genome (Wallberg et al. 2019) and
572 processed and filtered in the same way as described above for the termite data (GATK
573 VariantFiltration with the limits QD<2, FS>25, MQ<40, MQRankSum<-4, MQRankSum>4,
574 ReadPosRankSum<-4, ReadPosRankSum>4, SOR>3, ExcessHet>5 and VCFtools to select bi-
575 allelic sites with mean read depth between 5-13, quality score >= 30, minor allele count >=2
576 and <=40% missing genotypes).

577 *Estimation of population recombination rate*

578 The recombination rate was estimated using the complete, interval and stat functions of
579 LDhat (https://github.com/auton1/Ldhat, downloaded 2023-04-19) (Auton and McVean
580 2007) with 10 million iterations, sampling every 5000th iteration, taking the first 20 samples
581 as burn-in.

582 We evaluated different block penalties (1, 5 and 20), where a lower value allows the
583 recombination rate to change more easily across the map. As there were only minor
584 differences between the results for both species, we decided to use a block penalty of 1 as
585 this has been used previously in similar studies (Wallberg et al. 2015; Jones et al. 2019).

586 The output from the LDhat stat program gives the value of the parameter ρ/kbp between
587 each pair of consecutive SNPs. Those values were converted to equally sized windows across
588 each scaffold, as well as the coordinates of individual genomic features, by taking a
589 weighted average of values from overlapping intervals. The *M. bellicosus* scaffolds contain a
590 few gaps of unknown size and the values between SNPs across such gaps were removed.

591 The parameter ρ estimated by LDhat is proportional to the recombination rate r and the
592 effective population size N_E, which in turn can be estimated based on the mutation rate μ
593 and the number of segregating sites, S. In order to convert ρ to r, the following equations
594 were used, where n is the number of haploid sequences. The number of segregating sites

595 was calculated before the filter on minor allele count >=2 was applied, as this filter likely
596 removes many true SNPs as well, which could affect the estimates.

597

598 θ_W was estimated for each sample using the equation below from (Watterson 1975):

599 $$\theta_W = K \Big/ \sum_{i=1}^{n-1} \frac{1}{i}$$

600 where *K* is the number of SNPs and *i* is the number of haploid genomes sampled. We used
601 the value of θ_W to estimate N_E using:

602 $$N_E = \frac{\theta}{4\mu}$$

603 where μ is the mutation rate. We estimated N_E using a range of mutation rates estimated
604 from other insect species (Keightley et al. 2009, 2014, 2015; Yang et al. 2015; Liu et al.
605 2017). We then estimated the recombination rate using the following equation, assuming a
606 range of values of N_E.

607 $$r = \frac{\rho}{4N_e}$$

608

609 *Cumulative plot of rho* ρ/kbp

610 A cumulative plot of the proportion of rho versus the proportion of the physical distance
611 along the genome was constructed based on the output from LDhat for the two termite
612 species and previously generated LDhat output for *A. mellifera* (Wallberg et al. 2015;
613 PRJNA236426). The ρ/kbp estimates between markers were placed in decreasing order
614 before multiplication with the respective physical distances between the markers. Then
615 cumulative sums were calculated for the ρ-values as well as the corresponding physical
616 distances and divided by the total genome-wide sums.

617 *k-mer enrichment in recombination hotspots*

618 In order to identify k-mers associated with elevated recombination rate, we defined
619 recombination hotspots as 2kb segments with at least five-fold elevated recombination rate
620 compared to the local background, as defined by 50 kb flanking up and downstream of the
621 segment, resulting in 40894 regions for *C. secundus*, and 39837 for *M. bellicosus.*

622 Then, we used these hotspots to search for motifs associated with elevated recombination
623 rate by comparing against an equivalent number of randomly chosen 2kb regions from the
624 rest of the genome. This was done using STREME 5.5.4 (Bailey 2021) using a minimum and
625 maximum size of k-mer of 8 and 20, (--minw 8 ; --maxw 20) and otherwise default options.
626 From all motifs with significant enrichment after adjusting for multiple testing, we then
627 considered only motifs present in more than 5% of all hotspots and an at least two-fold
628 enrichment compared to the background as credible candidates.

629 *Identifying PRDM9 orthologues in C. secundus and M. bellicosus*

630 A full-length copy of PRDM9 is present in the *C. secundus* genome annotation, but not in *M.*
631 *bellicosus*. Using Orthofinder (Emms and Kelly 2019), and the genome annotation files for

632 both species, we identified a single orthologue to the *C. secundus* PRDM9 in *M. bellicosus*.
633 We analysed this region using the NCBI conserved domain search (Wang et al. 2023). We
634 also searched the *M. bellicosus* assembly for the PR/SET domains derived from *C. secundus*
635 and *Zootermopsis nevadensis* using BLAST (Camacho et al. 2009) and subsequently for all
636 other PRDM9 domains (KRAB, SSXRD, ZF-Casette) to identify hits that contain all other
637 PRDM9 domains in the vicinity in the correct order.

638 *Predicting binding sites from zinc-finger-motifs*

639 Using the ZF-motifs from *C.secundus,* we obtained letter probability matrices for predicted
640 binding motifs using a webserver (http://zf.princeton.edu/index.php ; (Persikov and Singh
641 2014) which were used to search for binding sites across the genome using FIMO (Grant et
642 al. 2011) with default options. Subsequently, the mean rho for the surrounding 1 kb bin was
643 used to test for a difference in mean rho between bins associated with a suspected binding
644 site, and a similar number of randomly chosen bins without association. For significance
645 testing, we repeated this draw 10.000 times to compare the associated bins against the 95%
646 confidence interval of the resulting distribution.

647 *Analysis of genomic correlates of recombination*

648 We divided the genome into 10 kb windows in which average ρ and other genomic features
649 were estimated. Windows shorter than 5 kb (half of the specified window size), which
650 appear in short scaffolds or at the ends at longer scaffolds, were excluded from the analyses
651 (excluding less than 1% of the sequence for each species). Correlation coefficients were
652 estimated with Spearmans ρ, with significance estimated by permutation tests with 10,000
653 iterations.

654 In order to determine the repeat content across the *C. secundus* and *M. bellicosus* genome
655 assemblies, we first generated custom repeat libraries for each species with RepeatModeler
656 (Flynn et al. 2020) using default options. This was then combined with Repbase 29 (Bao et
657 al. 2015) and DFAM 3.8 (Storer et al. 2021) and used to run RepeatMasker with default
658 options on each genome. We estimated the proportion of sequence in each repeat class in
659 10 kbp windows and used Spearman's rank correlation to correlate this with estimates of
660 recombination rate.

661 *Per gene recombination rate and $CpG_{O/E}$ ratio*

662 The observed/expected frequency of CpG sites ($CpG_{O/E}$) and mean ρ were calculated on a
663 per-gene basis, as well as for exons and introns, and 50kb flanking regions 10kb upstream
664 and downstream of the gene, akin to Wallberg et al (2015). For recombination rate, the data
665 from the interval function in LDhat (Auton and McVean 2007) was used, utilising a weighted
666 mean when the element spanned multiple markers. For visualisation, extreme $CpG_{O/E}$ values
667 due to low GC content were set to a maximum of 4.

668 We tested for significant difference in mean between ρ and $CpG_{O/E}$ in flanking regions, exons
669 and introns using paired t-tests corrected for multiple testing using a Bonferroni threshold.

670 *Differential expression data*

671 We classified genes in both species according to their caste-biased patterns of expression
672 from two studies (Elsner et al. 2018; Lin et al. 2021). Elsner et al. (2018) analysed four castes
673 of *M. bellicosus*, with two age classes of each: major and minor workers, queens and kings.
674 They analysed differences in gene expression among these classes using RNAseq data. We

reclassified the differential expression data by grouping the direct caste-vs-caste comparisons as "queen-biased", “king-biased”, “worker-biased”, “reproduction-biased”, "male-biased" or "female-biased" if they were differentially upregulated for this caste (or group) in comparison to other castes (or groups). Since Elser *et al.* (2018) initially mapped the *M. bellicosus* reads against the *Macrotermes natalensis* genome, We used orthofinder (Emms and Kelly 2019) to identify the *M. bellicosus* orthologues corresponding to the differentially expressed genes. Only single-copy genes were considered for this analysis.

Lin et al. (2021), performed RNAseq on samples of workers and queens. Here, we used the data from untreated queens and workers. Differentially expressed *C. secundus* genes were classified as “worker-biased” or “queen-biased” if they were differentially expressed with a bias to the respective caste, or unbiased if they were not, and subsequently compared between classes.

Correlates of recombination rate variation among genes

In order to assess the relative importance of $CpG_{O/E}$ ratio and differential expression patterns on recombination rate among genes, an ordinary least squares model was built using statsmodels (Seabold and Perktold 2010). $CpG_{O/E}$, differential expression categories, flanking regions $CpG_{O/E}$ and flanking region recombination rate were used as exogenous variables.

Data access

The scripts are available on GitHub: https://github.com/troe27/termite-recombination-rate. Raw sequence from population sequencing are available at NCBI BioProject PRJNA1021607.

Competing interest statement

The authors declare no competing interests.

Acknowledgements

We acknowledge grant 2018-03896 from The Swedish Research Council to MTW and from the Deutsche Forschungsgemeinschaft (DFG) KO-1895/26-1: 417980976 to JK. We acknowledge support from the National Genomics Infrastructure in Stockholm funded by Science for Life Laboratory, the Knut and Alice Wallenberg Foundation and the Swedish Research Council. The computations were enabled by resources in project NAISS 2023/23-402 provided by the National Academic Infrastructure for Supercomputing in Sweden (NAISS) at UPPMAX, funded by the Swedish Research Council through grant agreement no. 2022-06725. We thank Göran Arnqvist for helpful discussions on the evolution of sex and recombination. The Parks and Wildlife Commission, Northern Territory, and the Department of the Environment, Water, Heritage and the Arts, Australia, gave permission to collect (Permit number 59044) and export (PWS2016-001559) the *C. secundus* termites. The Office Ivoirien des Parcs et Réserves (OIPR) provided sampling and export permits for the *M. bellicosus* samples. The study was conducted according to the Nagoya protocol.

716 **References**

717 Agrawal AF. 2001. Sexual selection and the maintenance of sexual reproduction. *Nature*
718 **411**: 692–695.

719 Arsala D, Wu X, Yi SV, Lynch JA. 2022. Dnmt1a is essential for gene body methylation and
720 the regulation of the zygotic genome in a wasp. *PLOS Genetics* **18**: e1010181.

721 Auton A, McVean G. 2007. Recombination rate estimation in the presence of hotspots.
722 *Genome Research* **17**: 1219–27.

723 Axelsson E, Webster MT, Ratnakumar A, Consortium L, Ponting CP, Lindblad-Toh K. 2012.
724 Death of PRDM9 coincides with stabilization of the recombination landscape in the
725 dog genome. *Genome Res* **22**: 51–63.

726 Baer B. 2005. Sexual selection in Apis bees. *Apidologie* **36**: 187–200.

727 Bailey TL. 2021. STREME: accurate and versatile sequence motif discovery. *Bioinformatics*
728 **37**: 2834–2840.

729 Baker Z, Schumer M, Haba Y, Bashkirova L, Holland C, Rosenthal GG, Przeworski M. 2017.
730 Repeated losses of PRDM9-directed recombination despite the conservation of
731 PRDM9 across vertebrates ed. B. De Massy. *eLife* **6**: e24133.

732 Bao W, Kojima KK, Kohany O. 2015. Repbase Update, a database of repetitive elements in
733 eukaryotic genomes. *Mobile DNA* **6**: 11.

734 Baudat F, Buard J, Grey C, Fledel-Alon A, Ober C, Przeworski M, Coop G, de Massy B. 2010.
735 PRDM9 is a major determinant of meiotic recombination hotspots in humans and
736 mice. *Science* **327**: 836–840.

737 Begun DJ, Aquadro CF. 1992. Levels of naturally occurring DNA polymorphism correlate with
738 recombination rates in D. melanogaster. *Nature* **356**: 519–520.

739 Berglund J, Quilez J, Arndt PF, Webster MT. 2014. Germline methylation patterns determine
740 the distribution of recombination events in the dog genome. *Genome Biol Evol* **7**:
741 522–530.

742 Bewick AJ, Sanchez Z, Mckinney EC, Moore AJ, Moore PJ, Schmitz RJ. 2019. Dnmt1 is
743 essential for egg production and embryo viability in the large milkweed bug,
744 Oncopeltus fasciatus. *Epigenetics & Chromatin* **12**: 6.

745 Beye M, Gattermeier I, Hasselmann M, Gempe T, Schioett M, Baines JF, Schlipalius D,
746 Mougel F, Emore C, Rueppell O, et al. 2006. Exceptionally high levels of
747 recombination across the honey bee genome. *Genome research* **16**: 1339–44.

748 Browning BL, Zhou Y, Browning SR. 2018. A One-Penny Imputed Genome from Next-
749 Generation Reference Panels. *The American Journal of Human Genetics* **103**: 338–
750 348.

751 Browning SR, Browning BL. 2007. Rapid and accurate haplotype phasing and missing-data
752 inference for whole-genome association studies by use of localized haplotype
753 clustering. *Am J Hum Genet* **81**: 1084–1097.

754 Burt A, Bell G, Harvey PH. 1991. Sex differences in recombination. *Journal of Evolutionary*
755 *Biology* **4**: 259–277.

756 Camacho C, Coulouris G, Avagyan V, Ma N, Papadopoulos J, Bealer K, Madden TL. 2009.
757 BLAST+: architecture and applications. *BMC Bioinformatics* **10**: 421.

758 Cardoso DC, Santos HG, Cristiano MP. 2018. The Ant Chromosome database – ACdb: an
759 online resource for ant (Hymenoptera: Formicidae) chromosome researchers.
760 *Myrmecological News* **27**: 87–91.

761 Chan AH, Jenkins PA, Song YS. 2012. Genome-Wide Fine-Scale Recombination Rate Variation
762 in Drosophila melanogaster. *PLOS Genetics* **8**: e1003090.

763 Coop G, Przeworski M. 2007. An evolutionary view of human recombination. *Nature reviews*
764 *Genetics* **8**: 23–34.

765 Cunha MS, Cardoso DC, Cristiano MP, de Oliveira Campos LA, Lopes DM. 2021. The Bee
766 Chromosome database (Hymenoptera: Apidae). *Apidologie* **52**: 493–502.

767 Elango N, Hunt BG, Goodisman MA, Yi SV. 2009. DNA methylation is widespread and
768 associated with differential gene expression in castes of the honeybee, Apis
769 mellifera. *Proceedings of the National Academy of Sciences of the United States of*
770 *America* **106**: 11206–11.

771 Elsner D, Meusemann K, Korb J. 2018. Longevity and transposon defense, the case of
772 termite reproductives. *PNAS* **115**: 5504–5509.

773 Emms DM, Kelly S. 2019. OrthoFinder: phylogenetic orthology inference for comparative
774 genomics. *Genome Biology* **20**: 238.

775 Fischer O, Schmid-Hempel P. 2005. Selection by parasites may increase host recombination
776 frequency. *Biol Lett* **1**: 193–195.

777 Flynn JM, Hubley R, Goubert C, Rosen J, Clark AG, Feschotte C, Smit AF. 2020.
778 RepeatModeler2 for automated genomic discovery of transposable element families.
779 *Proceedings of the National Academy of Sciences* **117**: 9451–9457.

780 Glastad KM, Hunt BG, Yi SV, Goodisman M a. D. 2011. DNA methylation in insects: on the
781 brink of the epigenomic era. *Insect Molecular Biology* **20**: 553–565.

782 Grant CE, Bailey TL, Noble WS. 2011. FIMO: scanning for occurrences of a given motif.
783 *Bioinformatics* **27**: 1017–1018.

784 Harrison MC, Jongepier E, Robertson HM, Arning N, Bitard-Feildel T, Chao H, Childers CP,
785 Dinh H, Doddapaneni H, Dugan S, et al. 2018. Hemimetabolous genomes reveal
786 molecular basis of termite eusociality. *Nature Ecology & Evolution* **2**: 557–566.

Hartfield M, Keightley PD. 2012. Current hypotheses for the evolution of sex and recombination. *Integrative Zoology* **7**: 192–209.

Hedrick PW, Parker JD. 1997. Evolutionary Genetics and Genetic Variation of Haplodiploids and X-Linked Genes. *Annual Review of Ecology and Systematics* **28**: 55–83.

Hoffmann K, Foster KR, Korb J. 2012. Nest value mediates reproductive decision making within termite societies. *Behavioral Ecology* **23**: 1203–1208.

Immler S. 2019. Haploid Selection in "Diploid" Organisms. *Annual Review of Ecology, Evolution, and Systematics* **50**: 219–236.

Janicke T, Häderer IK, Lajeunesse MJ, Anthes N. 2016. Darwinian sex roles confirmed across the animal kingdom. *Science Advances* **2**: e1500983.

Jankásek M, Kotyková Varadínová Z, Šťáhlavský F. 2021. Blattodea Karyotype Database. *EJE* **118**: 192–199.

Jones JC, Wallberg A, Christmas MJ, Kapheim KM, Webster MT. 2019. Extreme Differences in Recombination Rate between the Genomes of a Solitary and a Social Bee. *Mol Biol Evol* **36**: 2277–2291.

Kawakami T, Wallberg A, Olsson A, Wintermantel D, de Miranda JR, Allsopp M, Rundlöf M, Webster MT. 2019. Substantial Heritable Variation in Recombination Rate on Multiple Scales in Honeybees and Bumblebees. *Genetics* **212**: 1101–1119.

Keightley PD, Ness RW, Halligan DL, Haddrill PR. 2014. Estimation of the Spontaneous Mutation Rate per Nucleotide Site in a Drosophila melanogaster Full-Sib Family. *Genetics* **196**: 313–320.

Keightley PD, Pinharanda A, Ness RW, Simpson F, Dasmahapatra KK, Mallet J, Davey JW, Jiggins CD. 2015. Estimation of the Spontaneous Mutation Rate in Heliconius melpomene. *Mol Biol Evol* **32**: 239–243.

Keightley PD, Trivedi U, Thomson M, Oliver F, Kumar S, Blaxter ML. 2009. Analysis of the genome sequences of three Drosophila melanogaster spontaneous mutation accumulation lines. *Genome Res* **19**: 1195–1201.

Kent CF, Minaei S, Harpur BA, Zayed A. 2012. Recombination is associated with the evolution of genome structure and worker behavior in honey bees. *PNAS* **109**: 18012–18017.

Kent CF, Zayed A. 2013. Evolution of recombination and genome structure in eusocial insects. *Communicative & Integrative Biology* **6**: e22919.

Koeniger G, Koeniger N, Phiancharoen M. 2011. Comparative Reproductive Biology of Honeybees. In *Honeybees of Asia* (eds. H.R. Hepburn and S.E. Radloff), pp. 159–206, Springer, Berlin, Heidelberg https://doi.org/10.1007/978-3-642-16422-4_8 (Accessed February 13, 2024).

823 Korb J. 2008. Termites, hemimetabolous diploid white ants? *Frontiers in Zoology* **5**: 15.

824 Korb J, Hartfelder K. 2008. Life history and development - a framework for understanding
825 developmental plasticity in lower termites. *Biological Reviews* **83**: 295–313.

826 Korb J, Thorne B. 2017. Sociality in Termites. In *Comparative Social Evolution* (eds. D.R.
827 Rubenstein and P. Abbot), pp. 124–153, Cambridge University Press, Cambridge
828 https://www.cambridge.org/core/books/comparative-social-evolution/sociality-in-
829 termites/11A80CB9FA947760889676E03899E85C (Accessed August 9, 2023).

830 Lam I, Keeney S. 2015. Nonparadoxical evolutionary stability of the recombination initiation
831 landscape in yeast. *Science* **350**: 932–937.

832 Leffler EM, Bullaughey K, Matute DR, Meyer WK, Ségurel L, Venkat A, Andolfatto P,
833 Przeworski M. 2012. Revisiting an Old Riddle: What Determines Genetic Diversity
834 Levels within Species? *PLoS Biol* **10**: e1001388.

835 Lenormand T. 2003. The evolution of sex dimorphism in recombination. *Genetics* **163**: 811–
836 22.

837 Lenormand T, Dutheil J. 2005. Recombination Difference between Sexes: A Role for Haploid
838 Selection. *PLoS Biology* **3**: e63.

839 Lin S, Werle J, Korb J. 2021. Transcriptomic analyses of the termite, Cryptotermes secundus,
840 reveal a gene network underlying a long lifespan and high fecundity. *Commun Biol* **4**:
841 1–12.

842 Liu H, Jia Y, Sun X, Tian D, Hurst LD, Yang S. 2017. Direct Determination of the Mutation Rate
843 in the Bumblebee Reveals Evidence for Weak Recombination-Associated Mutation
844 and an Approximate Rate Constancy in Insects. *Mol Biol Evol* **34**: 119–130.

845 Liu H, Zhang X, Huang J, Chen J-Q, Tian D, Hurst LD, Yang S. 2015. Causes and consequences
846 of crossing-over evidenced via a high-resolution recombinational landscape of the
847 honey bee. *Genome Biol* **16**: 15.

848 Lyko F, Foret S, Kucharski R, Wolf S, Falckenhayn C, Maleszka R. 2010. The Honey Bee
849 Epigenomes: Differential Methylation of Brain DNA in Queens and Workers. *PLoS Biol*
850 **8**: e1000506.

851 Misof B, Liu S, Meusemann K, Peters RS, Donath A, Mayer C, Frandsen PB, Ware J, Flouri T,
852 Beutel RG, et al. 2014. Phylogenomics resolves the timing and pattern of insect
853 evolution. *Science* **346**: 763–767.

854 Myers S, Bottolo L, Freeman C, McVean G, Donnelly P. 2005. A fine-scale map of
855 recombination rates and hotspots across the human genome. *Science* **310**: 321–4.

856 Myers S, Bowden R, Tumian A, Bontrop RE, Freeman C, Macfie TS, McVean G, Donnelly P.
857 2010. Drive against hotspot motifs in primates implicates the PRDM9 gene in meiotic
858 recombination. *Science* **327**: 876–9.

859 Nachman MW. 2001. Single nucleotide polymorphisms and recombination rate in humans.
860 *Trends in genetics : TIG* **17**: 481–5.

861 Niehuis O, Gibson JD, Rosenberg MS, Pannebakker BA, Koevoets T, Judson AK, Desjardins
862 CA, Kennedy K, Duggan D, Beukeboom LW, et al. 2010. Recombination and Its Impact
863 on the Genome of the Haplodiploid Parasitoid Wasp Nasonia. *PLOS ONE* **5**: e8597.

864 Parvanov ED, Petkov PM, Paigen K. 2010. Prdm9 controls activation of mammalian
865 recombination hotspots. *Science* **327**: 835–835.

866 Persikov AV, Singh M. 2014. De novo prediction of DNA-binding specificities for Cys2His2
867 zinc finger proteins. *Nucleic Acids Research* **42**: 97–108.

868 Qiu B, Elsner D, Korb J. 2023. High-quality long-read genome assemblies reveal evolutionary
869 patterns of transposable elements and DNA methylation in termites.
870 2023.10.31.564968.
871 https://www.biorxiv.org/content/10.1101/2023.10.31.564968v1 (Accessed January
872 8, 2024).

873 Roisin Y. 2001. Caste sex ratios, sex linkage, and reproductive strategies in termites. *Insectes*
874 *soc* **48**: 224–230.

875 Romiguier J, Lourenco J, Gayral P, Faivre N, Weinert LA, Ravel S, Ballenghien M, Cahais V,
876 Bernard A, Loire E, et al. 2014. Population genomics of eusocial insects: the costs of a
877 vertebrate-like effective population size. *Journal of Evolutionary Biology* **27**: 593–
878 603.

879 Ross L, Blackmon H, Lorite P, Gokhman VE, Hardy NB. 2015. Recombination, chromosome
880 number and eusociality in the Hymenoptera. *Journal of Evolutionary Biology* **28**:
881 105–116.

882 Rueppell O, Kuster R, Miller K, Fouks B, Rubio Correa S, Collazo J, Phaincharoen M, Tingek S,
883 Koeniger N. 2016. A New Metazoan Recombination Rate Record and Consistently
884 High Recombination Rates in the Honey Bee Genus Apis Accompanied by Frequent
885 Inversions but Not Translocations. *Genome Biol Evol* **8**: 3653–3660.

886 Sarda S, Zeng J, Hunt BG, Yi SV. 2012. The Evolution of Invertebrate Gene Body Methylation.
887 *Mol Biol Evol* **29**: 1907–1916.

888 Seabold S, Perktold J. 2010. Statsmodels: Econometric and Statistical Modeling with Python.
889 In *Proceedings of the 9th Python in Science Conference* (eds. S. Van der Walt and J.
890 Millman), pp. 92–96.

891 Sherman PW. 1979. Insect Chromosome Numbers and Eusociality. *The American Naturalist*
892 **113**: 925–935.

893 Shi YY, Sun LX, Huang ZY, Wu XB, Zhu YQ, Zheng HJ, Zeng ZJ. 2013. A SNP Based High-Density
894 Linkage Map of Apis cerana Reveals a High Recombination Rate Similar to Apis
895 mellifera. *PLOS ONE* **8**: e76459.

896 Siller S. 2001. Sexual selection and the maintenance of sex. *Nature* **411**: 689–692.

897 Singhal S, Leffler EM, Sannareddy K, Turner I, Venn O, Hooper DM, Strand AI, Li Q, Raney B,
898 Balakrishnan CN, et al. 2015. Stable recombination hotspots in birds. *Science* **350**:
899 928–932.

900 Sirviö A, Gadau J, Rueppell O, Lamatsch D, Boomsma JJ, Pamilo P, PAGE Jr. RE. 2006. High
901 recombination frequency creates genotypic diversity in colonies of the leaf-cutting
902 ant Acromyrmex echinatior. *Journal of Evolutionary Biology* **19**: 1475–1485.

903 Sirviö A, Johnston JS, Wenseleers T, Pamilo P. 2011a. A high recombination rate in eusocial
904 Hymenoptera: evidence from the common wasp Vespula vulgaris. *BMC Genetics* **12**:
905 95.

906 Sirviö A, Pamilo P, Johnson RA, Page Jr Robert E, Gadau J. 2011b. ORIGIN AND EVOLUTION
907 OF THE DEPENDENT LINEAGES IN THE GENETIC CASTE DETERMINATION SYSTEM OF
908 POGONOMYRMEX ANTS. *Evolution* **65**: 869–884.

909 Smukowski Heil CS, Ellison C, Dubin M, Noor MAF. 2015. Recombining without Hotspots: A
910 Comprehensive Evolutionary Portrait of Recombination in Two Closely Related
911 Species of Drosophila. *Genome Biology and Evolution* **7**: 2829–2842.

912 Stapley J, Feulner PGD, Johnston SE, Santure AW, Smadja CM. 2017. Variation in
913 recombination frequency and distribution across eukaryotes: patterns and
914 processes. *Philosophical Transactions of the Royal Society B: Biological Sciences* **372**:
915 20160455.

916 Storer J, Hubley R, Rosen J, Wheeler TJ, Smit AF. 2021. The Dfam community resource of
917 transposable element families, sequence models, and genome annotations. *Mobile*
918 *DNA* **12**: 2.

919 Templeton AR. 1979. Chromosome Number, Quantitative Genetics and Eusociality. *The*
920 *American Naturalist* **113**: 937–941.

921 Torres AP i, Höök L, Näsvall K, Shipilina D, Wiklund C, Vila R, Pruisscher P, Backström N.
922 2023. The fine-scale recombination rate variation and associations with genomic
923 features in a butterfly. *Genome Res* **33**: 810–823.

924 Trivers R. 1988. Sex differences in rates of recombination and sexual selection. In *The*
925 *Evolution of Sex*, pp. 270–286, Sinauer Associates, Sunderland, MA.

926 Trivers RL, Hare H. 1976. Haploidploidy and the Evolution of the Social Insect. *Science* **191**:
927 249–263.

928 Ventós-Alfonso A, Ylla G, Montañes J-C, Belles X. 2020. DNMT1 Promotes Genome
929 Methylation and Early Embryo Development in Cockroaches. *iScience* **23**: 101778.

930 Waiker P, de Abreu FCP, Luna-Lucena D, Freitas FCP, Simões ZLP, Rueppell O. 2021.
931 Recombination mapping of the Brazilian stingless bee Frieseomelitta varia confirms
932 high recombination rates in social hymenoptera. *BMC Genomics* **22**: 673.

933 Wallberg A, Bunikis I, Pettersson OV, Mosbech M-B, Childers AK, Evans JD, Mikheyev AS,
934 Robertson HM, Robinson GE, Webster MT. 2019. A hybrid de novo genome assembly
935 of the honeybee, Apis mellifera, with chromosome-length scaffolds. *BMC Genomics*
936 **20**: 275.

937 Wallberg A, Glémin S, Webster MT. 2015. Extreme recombination frequencies shape
938 genome variation and evolution in the honeybee, *Apis mellifera*. *PLoS Genetics* **11**:
939 e1005189.

940 Wallberg A, Han F, Wellhagen G, Dahle B, Kawata M, Haddad N, Simões ZLP, Allsopp MH,
941 Kandemir I, De la Rúa P, et al. 2014. A worldwide survey of genome sequence
942 variation provides insight into the evolutionary history of the honeybee *Apis*
943 *mellifera*. *Nat Genet* **46**: 1081–1088.

944 Wallberg A, Schöning C, Webster MT, Hasselmann M. 2017. Two extended haplotype blocks
945 are associated with adaptation to high altitude habitats in East African honey bees.
946 *PLoS Genetics* **13**: e1006792.

947 Wang J, Chitsaz F, Derbyshire MK, Gonzales NR, Gwadz M, Lu S, Marchler GH, Song JS,
948 Thanki N, Yamashita RA, et al. 2023. The conserved domain database in 2023.
949 *Nucleic Acids Res* **51**: D384–D388.

950 Wang X, Wheeler D, Avery A, Rago A, Choi J-H, Colbourne JK, Clark AG, Werren JH. 2013.
951 Function and Evolution of DNA Methylation in Nasonia vitripennis. *PLoS Genet* **9**:
952 e1003872.

953 Watterson GA. 1975. On the number of segregating sites in genetical models without
954 recombination. *Theoretical Population Biology* **7**: 256–276.

955 Wilfert L, Gadau J, Schmid-Hempel P. 2007. Variation in genomic recombination rates
956 among animal taxa and the case of social insects. *Heredity (Edinb)* **98**: 189–197.

957 Winkler L, Moiron M, Morrow EH, Janicke T. 2021. Stronger net selection on males across
958 animals eds. P.J. Wittkopp and L. Holman. *eLife* **10**: e68316.

959 Winston ML. 1991. *The Biology of the Honey Bee*. Revised edition. Harvard University Press,
960 Cambridge, Mass.

961 Wu T-C, Lichten M. 1994. Meiosis-Induced Double-Strand Break Sites Determined by Yeast
962 Chromatin Structure. *Science* **263**: 515–518.

963 Yang S, Wang L, Huang J, Zhang X, Yuan Y, Chen J-Q, Hurst LD, Tian D. 2015. Parent–progeny
964 sequencing indicates higher mutation rates in heterozygotes. *Nature* **523**: 463–467.

Zhang C, Dong S-S, Xu J-Y, He W-M, Yang T-L. 2019. PopLDdecay: a fast and effective tool for linkage disequilibrium decay analysis based on variant call format files. *Bioinformatics* **35**: 1786–1788.

Table 1. Estimates of levels genetic variation, effective population size and recombination rate in two termite species.

Species	Assembly length (Mb)	No. SNPs	θ_W/bp	ρ/kb	μ bp^{-1} gen^{-1}	N_E	r (cM/Mb)
M. bellicosus	1,139	5,581,662	0.14%	1.69	2.8	123,292	0.34
					3.5	98,634	0.43
C. secundus	992	15,037,468	0.44%	4.85	2.8	393,662	0.31
					3.5	314,930	0.38

θ_W/bp - Watterson's θ per base pair

ρ/kb - population recombination parameter, ρ, per kilobase

μ bp^{-1} gen^{-1} - estimate of mutation rate per base pair per generation

N_E - effective population size

r (cM/Mb) - recombination rate in centimorgans per megabase

979

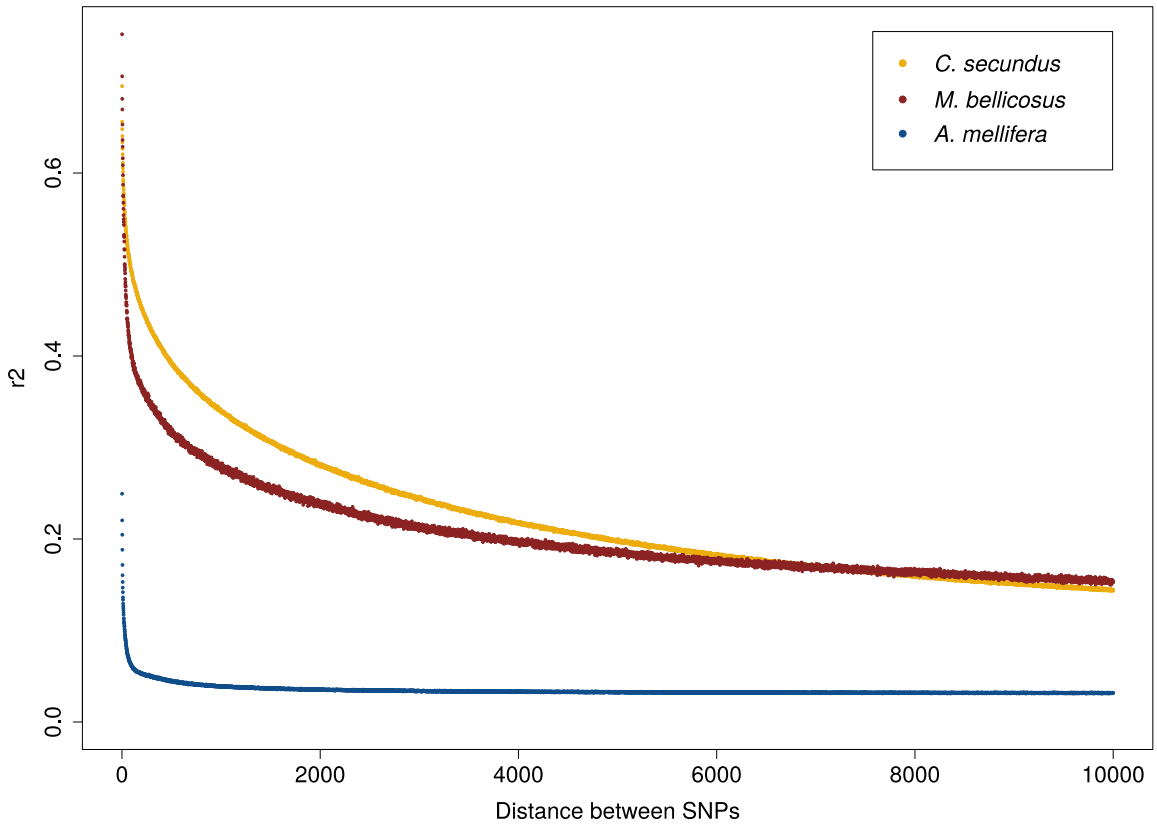

980

981

982 **Figure 1.** Genome-wide decay of LD measured as r^2 versus distance (bp) between SNPs for
983 the two termite species (*C. secundus*, yellow; *M. bellicosus*, dark red) and honey bees (*A.*
984 *mellifera scutellata*, blue; data from Wallberg et al. 2017).

985

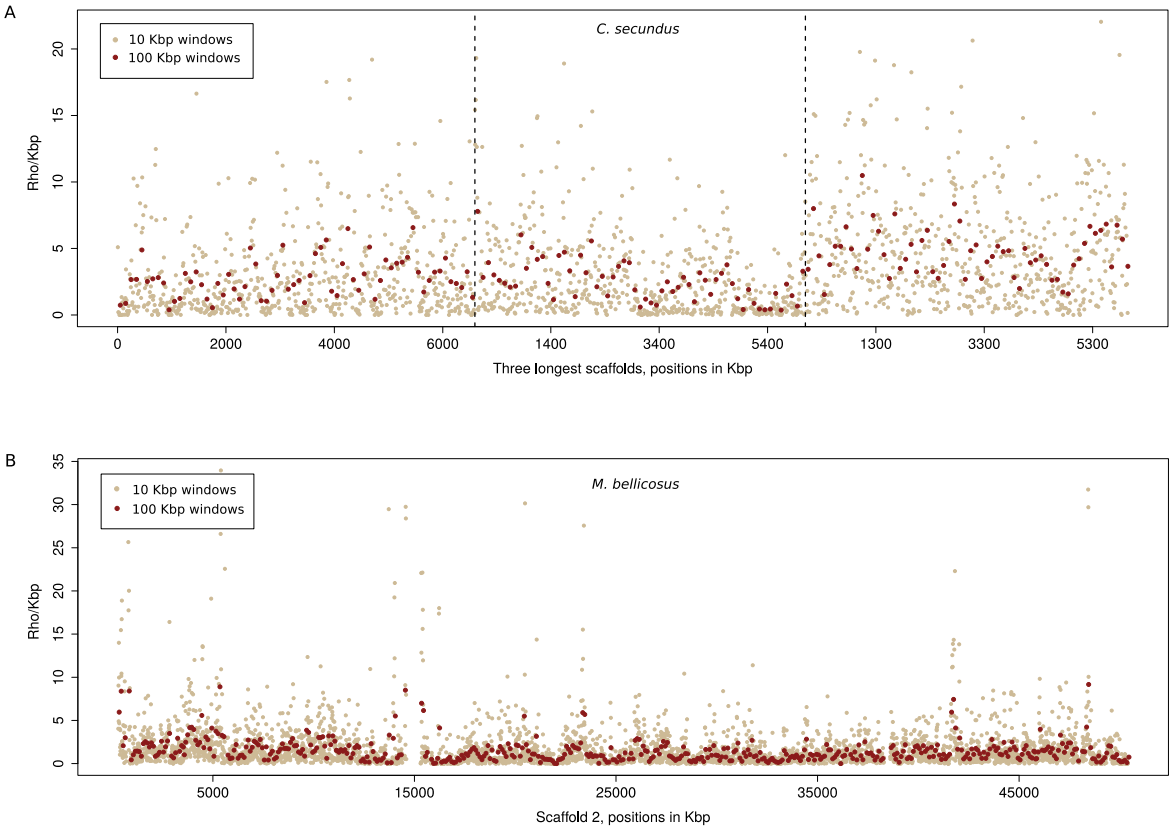

Figure 2. Variation in recombination rate estimated a ρ/kbp across representative genomic scaffolds in a) *C. secundus* and b) *M. bellicosus*. Estimates of ρ/kbp are calculated in 10 Kbp and 100 Kbp windows.

994

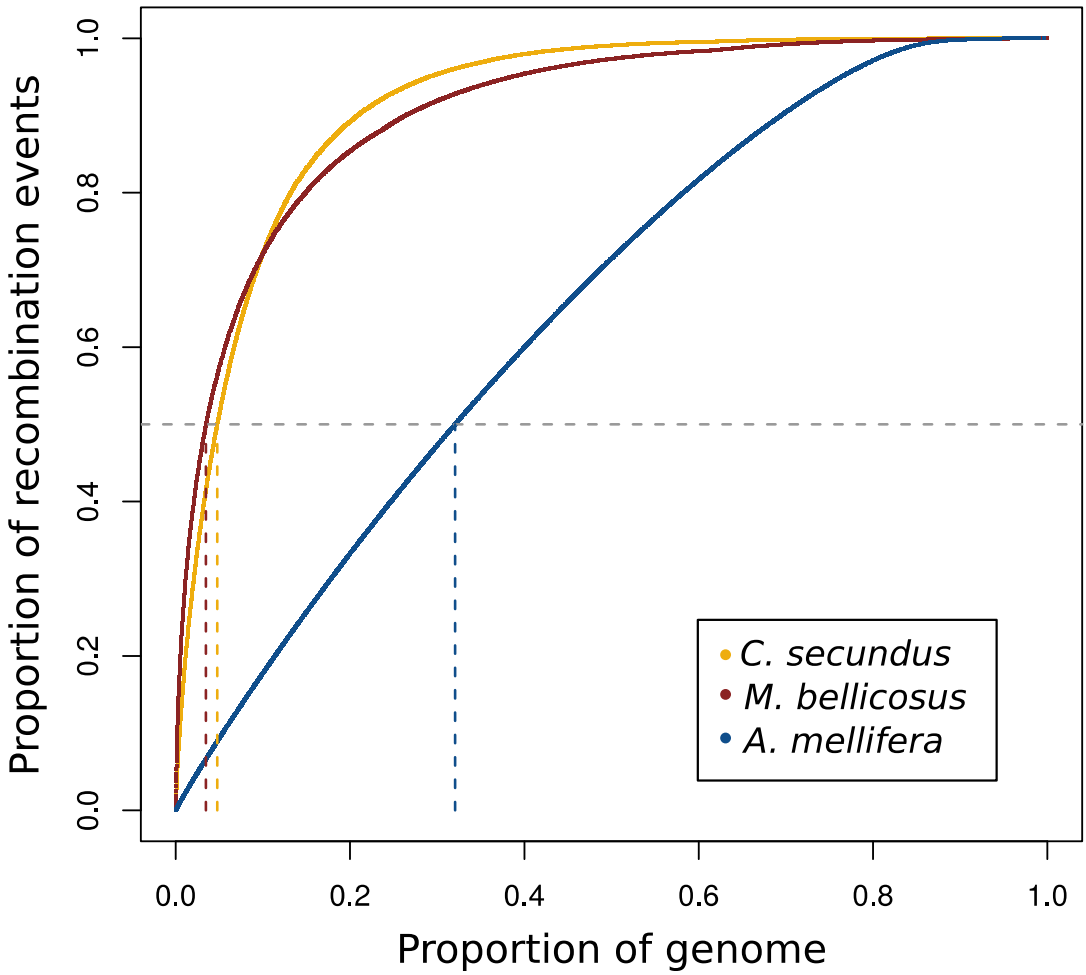

995

996

997 **Figure 3.** Cumulative plot of proportion of recombination events versus proportion of the
998 genome for the two termite species *C. secundus* and *M. bellicosus* compared to the honey
999 bee *A. mellifera* (Wallberg et al. 2015). Dashed lines show the proportion of the genome
1000 where 50 % of the recombination occurs, which for *C. secundus* is 4.77 %, *M. bellicosus* is
1001 3.47 % and *A. mellifera* is 32.05 %.

1002

1003

1004

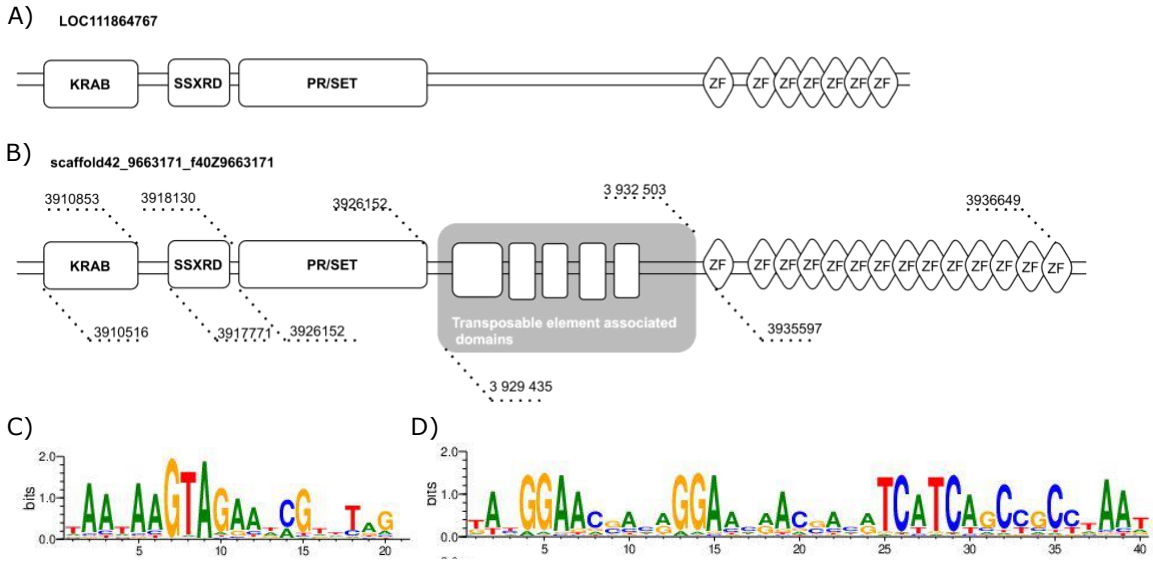

1005

1006

1007 **Figure 4.** PRMD9 structure and predicted zinc-finger motifs. A) Structure of PRDM9 in *C.*
1008 *secundus* genome annotation, B) predicted structure of PRDM9 in *M. bellicosus* identified by
1009 homology searches. C) predicted zinc finger binding motif in *C. secundus*, D) predicted zinc
1010 finger binding motif in *M. bellicosus*.

1011

1012

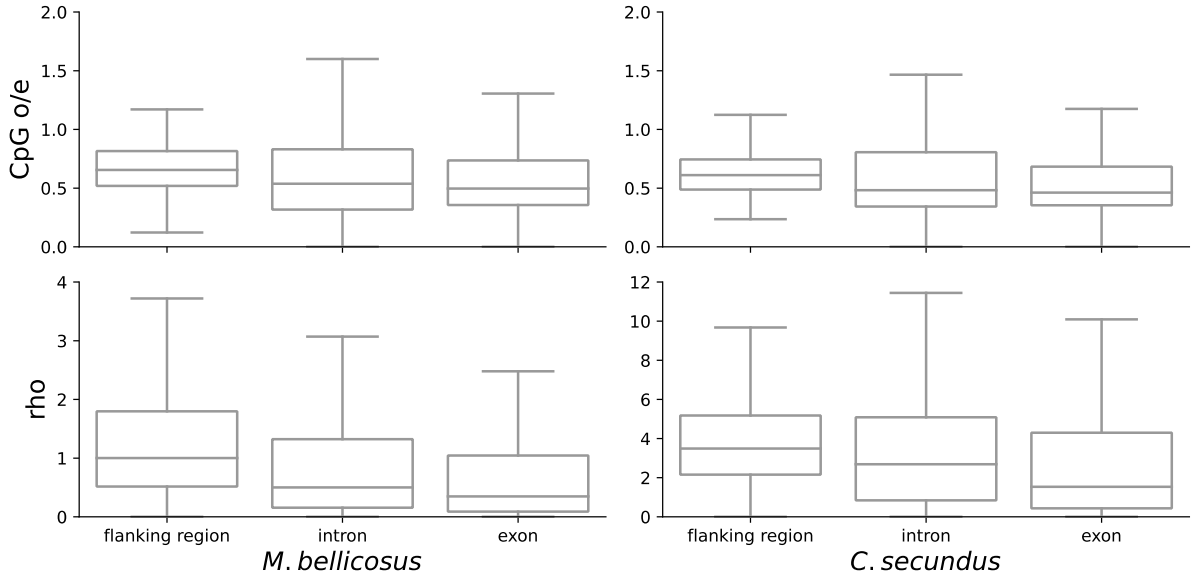

Figure 5. Boxplots showing variation in levels of $CpG_{O/E}$ and recombination rate (ρ/kbp; rho) in genic and flanking regions in the *M. bellicosus* and *C. secundus* genomes. The differences between all categories are significant.

Figure 6. Boxplots showing variation in levels of $CpG_{O/E}$ and recombination rate (ρ/kbp) in the coding region of genes in the *M. bellicosus* and *C. secundus* genomes classified according to their patterns of gene expression (Q = queen-biased, K = king-biased, W = worker-biased, F = female-biased, R = reproductive-biased).